Intra-ring variability of Cr, As, Cd, and Pb in red oak revealed by secondary ion mass spectrometry: Implications for environmental biomonitoring

D. J. Brabander, N. Keon, R. H. R. Stanley, and H. F. Hemond

PNAS 1999;96;14635-14640
doi:10.1073/pnas.96.25.14635

Intra-ring variability of Cr, As, Cd, and Pb in red oak revealed by secondary ion mass spectrometry: Implications for environmental biomonitoring

D. J. Brabander†, N. Keon, R. H. R. Stanley, and H. F. Hemond

Ralph M. Parsons Laboratory, Department of Civil and Environmental Engineering, Massachusetts Institute of Technology, Cambridge, MA 02139

Communicated by Stanley R. Hart, Woods Hole Oceanographic Institution, Woods Hole, MA, September 16, 1999 (received for review March 25, 1999)

Reconstructing the history of ambient levels of metals by using tree-ring chemistry is controversial. This controversy can be resolved in part through the use of selective microanalysis of individual wood cells. Using a combination of instrumental neutron activation analysis and secondary ion mass spectrometry, we have observed systematic inhomogeneity in the abundance of toxic metals (Cr, As, Cd, and Pb) within annual growth rings of *Quercus rubra* (red oak) and have characterized individual xylem members responsible for introducing micrometer-scale gradients in toxic metal abundances. These gradients are useful for placing constraints on both the magnitude and the mechanism of heavy metal translocation within growing wood. It should now be possible to test, on a metal-by-metal basis, the suitability of using tree-ring chemistries for deciphering long-term records of many environmental metals.

Materials such as continental ice and lake, ocean, and wetland sediments are currently used to develop records of past chemical conditions. However, the geographic distribution of suitable deposits is limited; furthermore, dating of these materials can be uncertain. Because of their relative ease of dating, large geographic range, and record length extending back to the preindustrial era, tree rings have long intrigued scientists from many disciplines as monitors of environmental conditions. Nearly three decades of work, however, have produced a literature that is highly polarized between those who have demonstrated that various tree species faithfully record and preserve records of environmental metal contamination and those who have documented that measured dendrochemical patterns of metals do not correlate with known changes in past environmental conditions (1).

We contend that the reasons for this polarization stem from our general inability to address several fundamental questions. What are the contaminant pathways of metals within the tree-soil–groundwater–atmosphere system? Is the uptake of nonessential metals proportional to ambient levels in the immediate environment of the tree? Once taken up into the stem wood, do the metals stay where they first interact with the xylem tissues or are they mobile? And finally, how long are these complex biogeochemical signals preserved within the stem wood? To determine the efficacy of using dendrochemical approaches to monitor metal loading histories, these processes that govern both the uptake and storage of metals within each potential biomonitoring species must be evaluated. In this paper, we propose methodologies that aid in quantifying these difficult-to-evaluate interdependent processes.

We believe the dichotomy of observations concerning the use of tree-ring chemistry to monitor metals is a consequence of two closely related underlying problems: an inadequate understanding of the physiological controls on the rates of metal translocation within trees, and a reliance on analytical approaches that require the complete digestion and hence homogenization of bulk wood tissues. Digestion techniques, which typically average signals over one or more annual growth increments, provide no information on the spatial heterogeneities within the various xylem tissue members (e.g., vessels within earlywood and latewood, ray and axial parenchyma, and nonconducting fibrous cells) of a single growth increment. Recent developments in sample preparation procedures and analytical instrumentation now allow the application of secondary ion mass spectrometry (SIMS) to a wide range of biological materials (2–4). SIMS permits *in situ* micrometer-scale analysis of toxic metal abundance directly within the various types of xylem members, making it possible to assess whether different xylem tissues record environmentally unique elemental signals.

We report on the systematic results from these methodologies to study the uptake and translocation of toxic trace metals in red oak (*Quercus rubra*) from a Superfund site in Woburn, MA. To elucidate micrometer-scale metal distribution, we conducted detailed analyses within single annual rings. Our results indicate that certain metals (e.g., Cr and As) are strongly concentrated in earlywood, whereas others (such as Pb, Cd, and Zn) are more uniformly distributed throughout the entire growth increment. Although other researchers have recently published observations on the seasonal variability of metal distributions within stem wood (5–9), the density of our data set and a unique analytical geometry allow us to use elemental patterns to place different constraints on metal translocation mechanisms, including effective diffusion coefficients, within the xylem. Ultimately, micrometer-scale inquiry can contribute to an understanding of the physiological controls on metal transport within trees and may make it possible to extract meaningful and interpretable long-term records of ambient levels of metals.

Environmental Monitoring via Tree-Ring Chemistry. Three *in situ* biogeochemical analytical methodologies, proton-induced x-ray emission, laser ablation inductively coupled plasma mass spectrometry, and SIMS, have sparked several studies (10–13) aimed at answering the long-standing question: how useful is the chemical information stored within tree rings for reconstructing past chemical environments? The literature contains many examples in which detailed dendrochemical records of both atmospheric- and groundwater-derived contamination events can be correlated with known source functions (14–16). However, an almost equal number of studies concluded that no correlation exists between pollution levels and tree-ring chemistry (17–19). Although all of the *in situ* biogeochemical analytical methodologies offer millimeter- to micrometer-scale spatial resolution, only SIMS and laser ablation inductively coupled plasma mass spectrometry combine this high spatial resolution with low detection limits (in the parts-per-billion range). We used the SIMS approach, because it has the additional capability of creating detailed three-dimensional maps of the relative

Abbreviations: SIMS, secondary ion mass spectrometry; INAA, instrumental neutron activation analysis; SEM, scanning electron microscope.

†To whom reprint requests should be addressed. E-mail: dbraband@mit.edu.

The publication costs of this article were defrayed in part by page charge payment. This article must therefore be hereby marked "*advertisement*" in accordance with 18 U.S.C. §1734 solely to indicate this fact.

elemental abundances in a continuous depth profiling mode that achieves submicrometer scale resolution (sufficient to analyze individual xylem tissue members). We present SIMS results for several toxic metals, including Cr, As, Cd, and Pb, but, in this paper, we focus on interpreting and modeling the observed micrometer-scale concentration gradients for Cr within oak stemwood.

Site Characterization. Cr is known to be a long-term anthropogenic contaminant within the 65-km^2 Aberjona watershed within greater metropolitan Boston (20, 21). Mass balance studies suggest that tanning and leather finishing industries released 200 to 400 tons of Cr solid waste and 2,000 to 4,000 tons of Cr wastewater into the watershed during the past century (22). Lake sediments document a long history of metal contamination (23), and elevated levels of phytochelatins (a biophysical indicator of metal stress) have been observed in trees at the Wells G & H Superfund site and elsewhere on the watershed (24). These data have been interpreted as evidence of present-day metal stress from exposure to metal-contaminated groundwater at the Wells G & H site where two municipal wells operated intermittently between 1964 and 1979. This location provides a unique opportunity to determine whether the red oak trees contain interpretable records of both long-term metal contamination of the watershed and possible short-term local events associated with the operation of the municipal wells.

Materials and Methods

Tree cores were taken at breast height with a standard forestry service 4-mm increment borer. The cores were placed in polyethylene bags, stored on ice until transport to the lab, and then stored at −80°C until sectioned. Each core was sectioned longitudinally with a slow-speed diamond wafering saw. After longitudinal sectioning, one half of the core was cut into annual increments, each of which was then subsectioned into earlywood and latewood with a Teflon-coated razor blade. These samples were analyzed by instrumental neutron activation analysis (INAA) at the Massachusetts Institute of Technology reactor facility. The other half of the core was analyzed by SIMS allowing direct comparison of two non-digestion-based analytical methods on the same core. The SIMS sections were cut into multiyear increments with a slow-speed diamond wafering saw, wrapped in aluminum foil, and mounted in a brass ring with room-temperature-curing Buehler epoxide resin. After curing, the protective aluminum foil was removed, revealing a surface that showed a high degree of tissue preservation. After coating with Au in a conventional evaporation apparatus, the surface was reflective enough for ion probe optical inspection and conductive enough to avoid serious charging problems. Rastered analyses and depth profiles were measured by using a Cameca IMS 3f ion microprobe (Paris) at the Woods Hole Oceanographic Institution regional facility. The analysis was performed with a primary beam of negatively charged oxygen ions accelerated to 8–9 keV (1 eV = 1.602×10^{-19} J) and primary beam currents in the range of 15–150 nA. Beam diameters ranged from 10 to 50 μm and were rastered over a rectangular area approximately 100–150 μm on a side. Count times for each metal isotope measured ranged from 20 to 30 s per cycle, whereas ^{16}O was counted for 5 s. To minimize isobaric interferences, various energy-filtering conditions (i.e., offset voltages; see ref. 25) were optimized for each element of interest until good agreement was achieved with natural isotopic abundances. These energy-filtering conditions ranged from −40 V for the Cr isotopes to −5 V for the Pb isotopes; all other elements were measured at −20 V (all with a 20-eV energy window). As a consequence, the intercomparison of the relative abundances of the measured metals is not feasible; however, the INAA data provide this information. The depths of the sputtered analysis craters were determined by using a Dektak 8000 profilometer (Santa Barbara, CA) and have a relative precision of ±5% of the total measured depth.

Results and Discussion

Fig. 1*a* illustrates a typical SIMS depth profile from earlywood; the optical and scanning electron microscope (SEM) photomicrographs (Fig. 1*b*) show analysis areas. The photographs confirm that the SIMS technique is capable of measuring metals in individual members. Fig. 1*a* plots the counts per second for each ion measured as a function of cycle number of analysis, which is proportional to depth in the wood. In all of the following SIMS figures, the vertical axes are the measured ratios of metal elemental ions to a reference, the $^{16}O^+$ ion, which is chosen as the reference element because it is subject only to minimal matrix effects. Analysis crater depths ranged from 10 to 150 μm. For each analysis, the last 6–12 cycles of data are averaged and reported. As shown in Fig. 1 *a* and *c* (for this analytical geometry), when a metal signal is normalized to oxygen, the result is a metal/oxygen (in this case $^{52}Cr/^{16}O$) profile with near-uniform isotopic ratios for the entire analysis, and expected natural isotopic abundances are observed. Plots of the metal/oxygen ratio versus absolute number of ^{16}O counts indicate no dependence on total number of counts collected for the normalizing element, supporting the choice of oxygen as an appropriate normalization element for an oak stem wood matrix.

In over 20 SIMS analyses of annual growth rings, Cr and As were found preferentially in the earlywood of each growth increment, whereas Cd and Pb were found to be more uniformly disseminated throughout the xylem tissues. It has been shown that vessel walls are ion exchangers and thus may be responsible for binding Cr and As at the vessel-wall–xylem-stream interface (26). Therefore, the bulk difference in the concentration between earlywood and latewood may be related to the larger volume of vessel elements within the earlywood.

To test this hypothesis and to determine whether the measured Cr/O SIMS ratios are a proxy for observing changes in Cr concentrations, a portion of the core was analyzed by both INAA and SIMS. Fig. 2*a* plots the INAA results for Cr (in nanograms per gram) for a 3-year time span from 1967–1969. It is apparent that Cr is distributed preferentially into the earlywood. Fig. 2*b* plots the SIMS results obtained from the same core over the time interval from earlywood 1968 to earlywood 1969. The *y* axis is the $^{52}Cr/^{16}O$ ratio, whereas the abscissa (in millimeters) denotes the actual location of the SIMS analysis within each growth increment. The SIMS data also illustrate a partitioning of Cr into the earlywood. Fig. 2*c* is a comparison of partitioning ratios defined as earlywood/latewood, determined by both analytical methods. For the INAA results, Cr ranged from 1.4 to 2.5 with an average partitioning ratio over this time interval of 1.9 ± 0.5 (all ratios' uncertainties are cited as 1 σ). Similar results were obtained for As (partitioning ratio = 1.7 ± 0.6) but are in stark contrast to the mobile macro-nutrient metals such as K, which showed essentially no partitioning between earlywood and latewood (partitioning ratio = 0.9 ± 0.1). The estimated earlywood/latewood ratio determined from the SIMS results for Cr in 1968 is 2.9 ± 0.9. Considering the tremendous range in area of wood analyzed by each technique (typically 6 mm^2 for INAA and 0.02 mm^2 for SIMS) the observed partitioning ratios suggest that both methods provide similar responses to changes in the concentration of Cr within the xylem tissue.

To test further the hypothesis that certain metals (such as Cr and As) are strongly associated with earlywood and in particular with the large vessel elements found only within the earlywood, we performed a series of SIMS spot analyses at varying distances from earlywood vessel elements from the 1968 growth increment. Fig. 3*a* shows the proximity of the analysis spots to the 100- to 200-μm diameter vessel elements. Fig. 3*b* plots the metal/

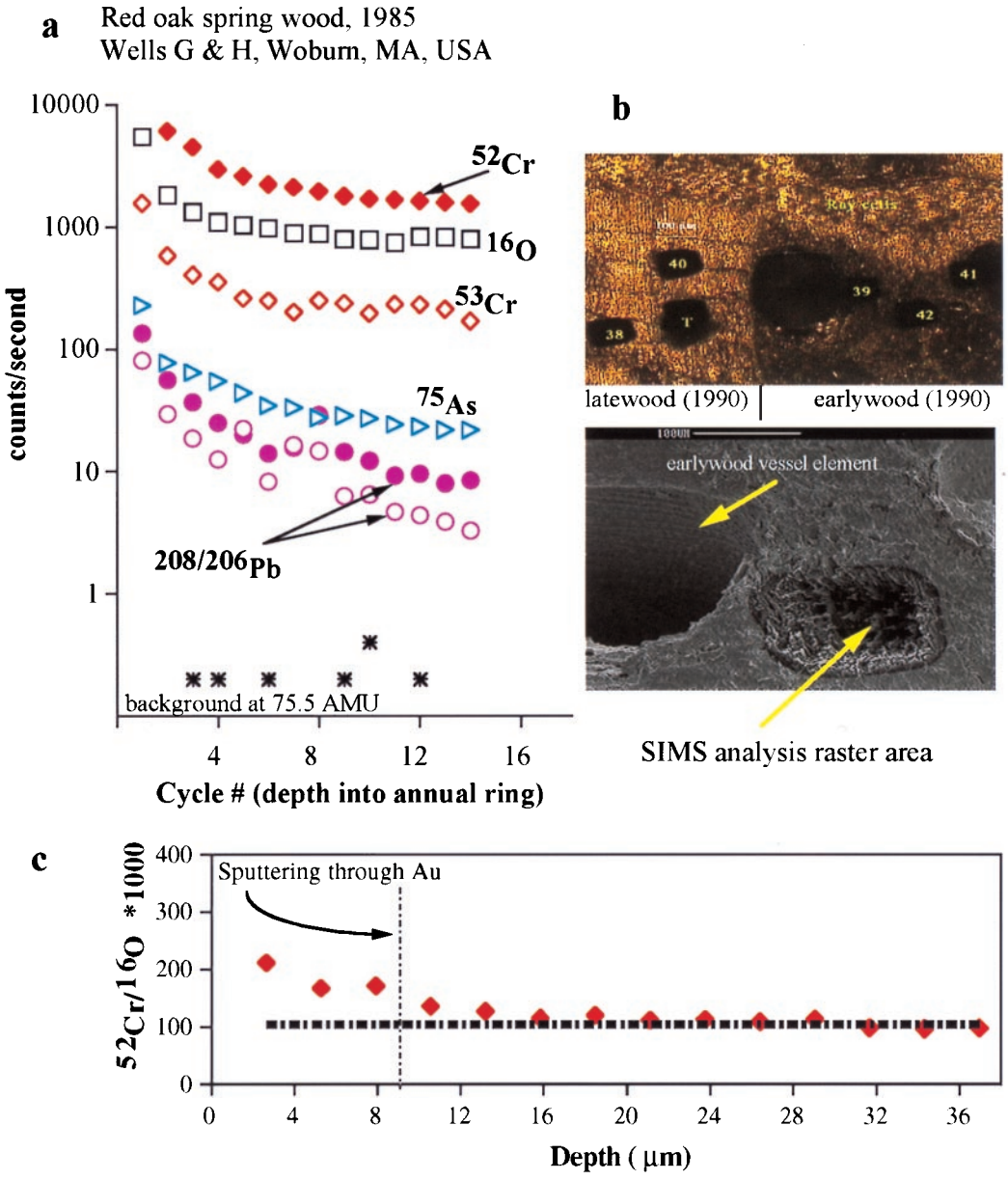

Fig. 1. Typical SIMS depth-profiling analysis. (*a*) All data are plotted as counts per second, except ^{52}Cr and ^{53}Cr, which, for clarity, are plotted as total counts collected during 20-s count periods. AMU, atomic mass units. (*b*) Optical and SEM photomicrographs illustrate spatial resolution of analyses with respect to xylem members. (*c*) Normalized $^{52}Cr/^{16}O$ ratios for the data presented in *a*. The first three analyses represent sputtering through the Au conductive coating, whereas the last six analyses are averaged to obtain representative metal/oxygen ratios denoted by the dashed horizontal line. Note cycle numbers from *a* have been converted to depth in micrometers (see *Results and Discussion* for details).

oxygen isotopic ratios for Cd, Pb, As, and Cr versus distance from the vessel wall. Several important conclusions are apparent. Pb and Cd lack a strong functional relationship with distance to the xylem. However, As and Cr increase as the vessel wall is approached, especially for analyses that fall between two closely spaced vessel elements (see analysis number four in As and Cr step scans). These results suggest that As and Cr, both known groundwater contaminants on this site, are biologically mobile and are taken up by red oak trees. Further, they seem to enter the wood through vessel walls first and then diffuse into the xylem tissue.

Finding clues to the kinetics governing metal migration within the earlywood requires spatial resolution beyond what is possible for the ion probe in the spot mode analytical condition. To improve radial resolution of these concentration gradients, we changed both sample geometry and SIMS analytical conditions such that very detailed analyses could be made longitudinally (at right angles) to individual vessel walls. SEM photomicrographs and a schematic diagram in Fig. 4*a* show how it is possible to analyze single vessel elements by cutting the tree core longitudinal to traditional growth-radial sections and operating the ion probe in the continuous depth-profiling mode. As the analysis progresses, the beam slowly sputters through the vessel wall and into earlywood. Recall from Fig. 3 that we observed the highest levels of Cr nearest to the vessel elements. Fig. 4*b* illustrates that Cr concentration within a vessel wall monotonically decreases with distance from the inside of the vessel wall. The depth of this profile measured with a profilometer (Dektak 8000) is 55 ± 5 μm.

The patterns observed on the year-to-year scale and between earlywood and latewood seem to originate in part with the trends

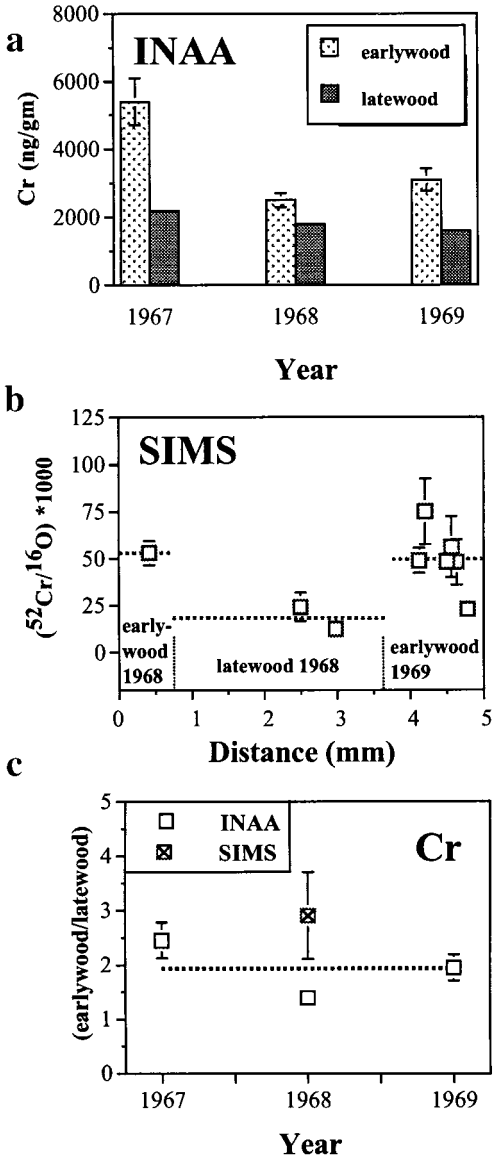

Fig. 2. SIMS and INAA analyses. (*a*) Earlywood and latewood Cr (in nanograms per gram) determined by INAA. The earlywood and latewood concentrations of Cr are statistically different at the 2-σ level, whereas error bars represent 1 σ. (*b*) Detailed set of SIMS analyses obtained during the earlywood 1969 to earlywood 1968 time period. The *x* axis represents the actual location of the SIMS analysis within each growth increment, and the dashed horizontal lines are the average ^{52}Cr/^{16}O ratio observed in each growth increment. (*c*) Comparison of earlywood/latewood partitioning ratios determined by SIMS and INAA.

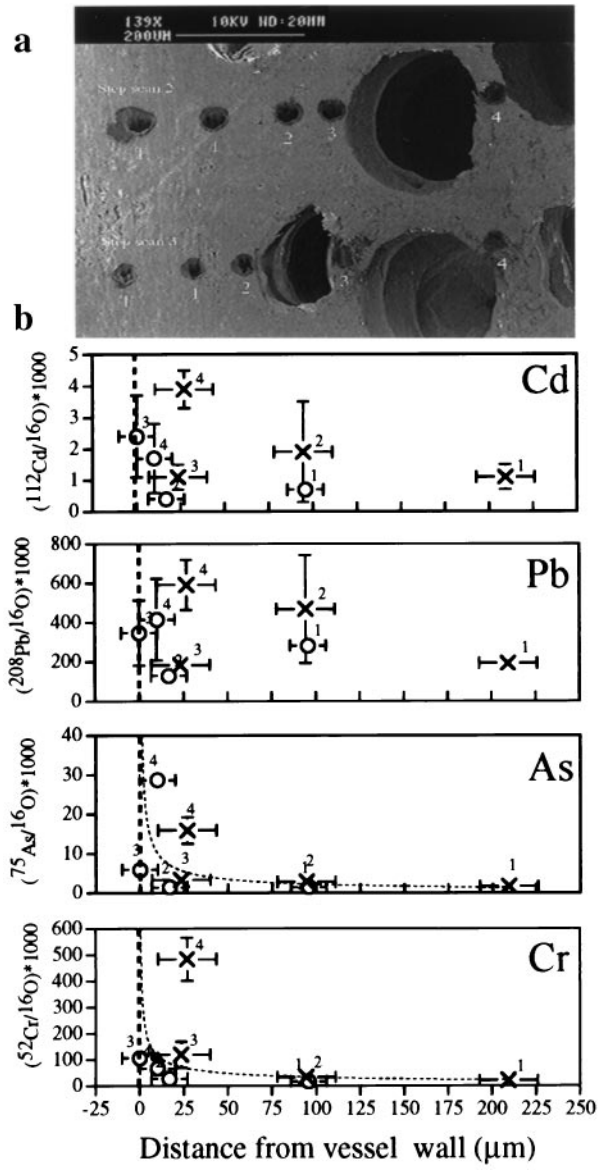

Fig. 3. SIMS step scan analyses. (*a*) SEM photomicrograph of spot analyses near vessel element in earlywood 1968. (*b*) Cd, Pb, As, and Cr ratios as a function of distance from the vessel wall. Note, two separate scans were made approaching different vessel elements within the same growth increment (× plot symbols indicate scan two, whereas ○ indicates scan three). Abscissa error bars are based on ion probe beam diameter, and ordinate error bars are based on the 1-σ variation about the mean of the cycles used to determine metal/oxygen ratio. Dashed lines for As and Cr are exponential curves fitted to the data.

observed within these vessel walls. As the distance from the inside wall of the vessel increases, the (Cr/O) *1,000 ratio decreases steadily, from approximately 300 to 100, a value typically observed for earlywood in this tree. This profile may provide direct evidence of a preserved down-gradient diffusive profile within xylem wood. The modeling of this profile is the subject of the next section.

Modeling Translocation Mechanism. If diffusive transport were responsible for generating the concentration profile of Cr shown in Fig. 3*b*, then the inverse error function of Cr concentration should be linearly proportional to depth into the vessel wall. Fig. 3*b* illustrates a test for this predicted relationship. The simplest model assumes that metal flow in the xylem stream produces a constant metal concentration at the fluid/xylem cell wall interface. Note that more complex boundary conditions would require data on the exact time course of metal concentration and the partitioning of the metal between the xylem fluid and cell wall. The "end" of the diffusion profile was chosen as the point at which the metal/oxygen ratio reached 100, a typically observed earlywood ratio (recall Fig. 1*c*). The data from the concentration profiles were modeled by using the solution to the diffusion equation given by Crank (27) for transport normal to the surface of a solid from a well stirred semiinfinite volume:

$$\frac{(C_x - C_1)}{(C_0 - C_1)} = \mathrm{erf}\left(\frac{x}{2\sqrt{Dt}}\right), \qquad [1]$$

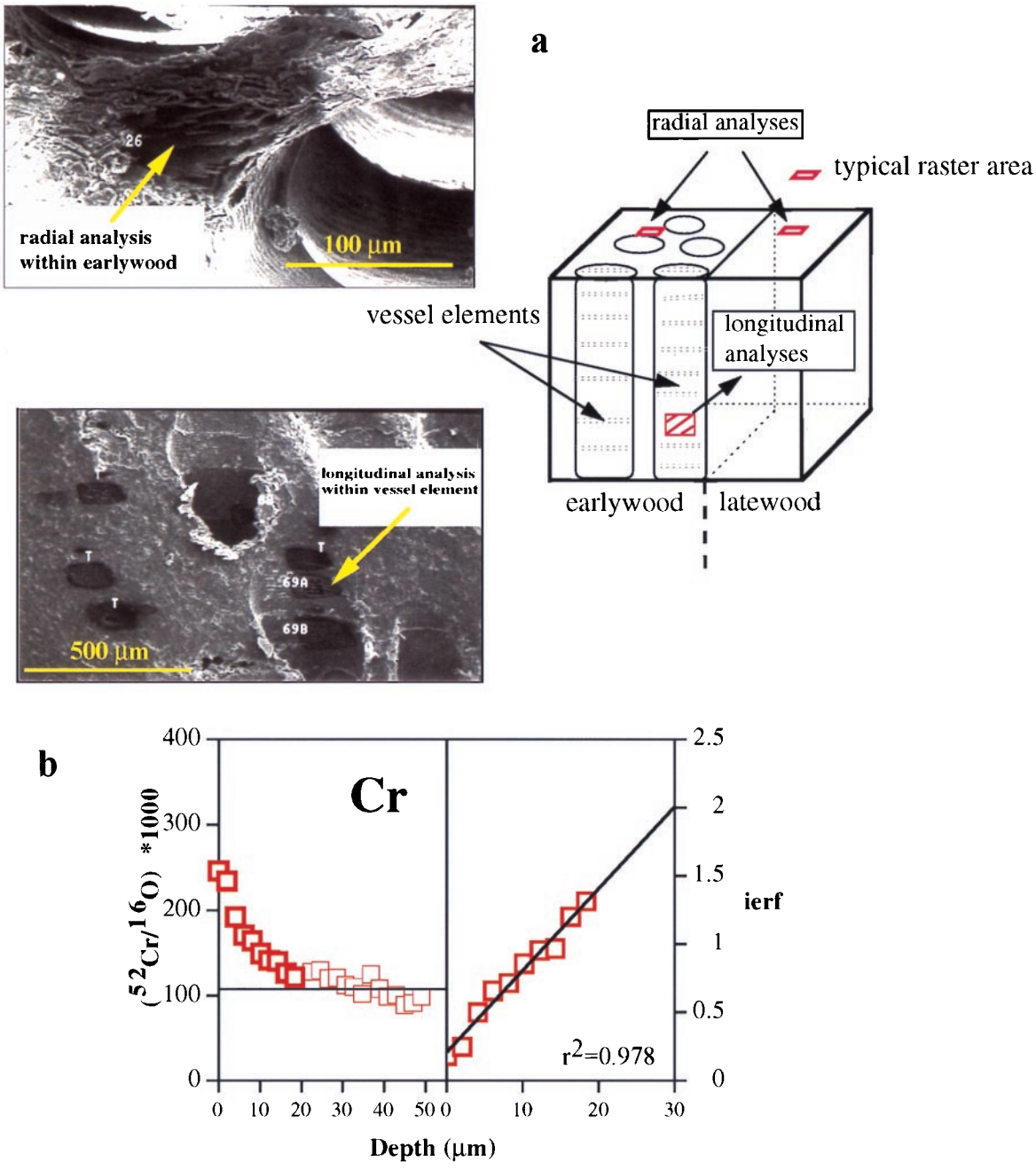

Fig. 4. SIMS *in situ* analysis geometries. (*a*) Analysis geometries as depicted by SEM photomicrographs in relation to schematic depiction of a single growth increment. (*b*) Cr SIMS depth profile analysis longitudinal to vessel element (Wells G & H, spring 1974, Woburn, MA). Depth into vessel wall increases along the *x* axis (total depth = 55 μm). The first two cycles of data were omitted as they represent sputtering through the Au conductive coating. Bold symbols are used to calculate values of the diffusion coefficient × time. Note the good fit to the inverse error function analysis (ierf).

where $C_x - C_1/C_0 - C_1$ is the reduced concentration, C_x is the concentration at a depth x, C_1 is the concentration at the surface, C_0 is the background concentration in the xylem tissue, D is the diffusion coefficient, t is time, and erf is the error function. (Note that, with these analyses, we cannot accurately determine the distribution coefficient between the aqueous solution and the solid tissue; however, as long as C_1 is constant during the time it takes to generate the concentration profile, it does not have bearing on the model used to calculate the D values). We applied a least squares linear regression to determine the slope of the line, which is proportional to $2\sqrt{Dt}$, where D is the effective diffusion coefficient. The good fit is consistent with diffusion being the primary mechanism of migration within the vessel wall xylem tissue. If competing translocation mechanisms operated during the time between the addition of this annual ring and sampling, such a close fit in the inverse error function modeling would seem unlikely.

Estimation of Diffusion Rates. To obtain D, one has to select an appropriate value for t, the time variable in Eq. **1**. Several logical choices can be argued. In the few cases of reported D values for metals in wood, the time used to calculate the diffusion coefficients is typically the time between the formation and sampling of the growth increment or ring. In the present case, this time

interval is 22 years, and the resulting D value is 1.0×10^{-15} cm^2/s. However, over 22 years, the wood tissues undergo physiological changes, and the boundary conditions for the solution to the diffusion equation also change as the vessel conduit becomes less conductive and further removed from the primary xylem fluid flow. Considering these changes, it seems unlikely that the observed Cr profile is the result of 22 years of input to the wood. Therefore, two alternative treatments are considered. One option is to consider the duration of time the wood sample resided within the more conductive sapwood. For this tree, the boundary between the sapwood and the heartwood takes place 8 years before the current growth increment. Substituting this time interval into Eq. **1** and solving for D we obtain 2.7×10^{-15} cm^2/s. However, studies show that over 90% of the xylem transport in ring-porous trees takes place in the single outermost growth ring (28). Therefore, it may be appropriate to consider only the 5-month time period during the active growth season as the time interval during which a single translocation mechanism is operating. If that is the case, then the calculated D becomes 5.2×10^{-14} cm^2/s, 52 times higher than the other extreme value. These D values are low enough that radial diffusion will not play a major role in modifying the dendrochemical record stored within tree rings. For example, by using the full range of the D calculated above, in 100 years, Cr would diffuse a minimum of 18 μm and a maximum of 128 μm. It is worth noting that, with our current measurements, it is not possible to determine whether the observed diffusion profiles were generated during a single growing season and then preserved (as the xylem tissues further lignify and the vessel elements no longer conduct the xylem stream) or whether the profiles were generated throughout the 22 year history of the growth increment. However, in either case, the predicted translocation of Cr by diffusion alone is limited to the modification of the concentration profiles within the width of a single growth increment.

Implications for Modeling Pollutant Pathways. We have demonstrated that red oak trees have certain necessary biophysical attributes to be effective groundwater biomonitors. *In situ* microanalytical techniques have identified the individual xylem members responsible for introducing small-scale heterogeneity in abundances of several toxic metals. This heterogeneity on an annual growth ring scale could introduce artifacts in dendrochemical records that, unless identified, might confound efforts to decipher historical records of Cr stored within the tree rings.

We contend that it is now possible not only to observe heterogeneities but to use them both for estimating metal translocation kinetics and for reconstructing the history of ambient metal levels within a local environment. The calculated D values in this study are low enough that, once written, environmental records from oak stem wood should be preserved for at least a century. In addition to quantifying the feasibility of dating contamination events with dendrochemical analysis, the unique spatial resolution of the SIMS technique has opened the door for the possibility of tracing the actual pathways of the metal contamination within the xylem wood.

We thank G. Layne and N. Shimizu at the Woods Hole Oceanographic Institution Northeast National Ion Microprobe Facility (supported by Grant EAR-9628749 from the National Science Foundation), Mike Ames at the Massachusetts Institute of Technology nuclear reactor facility, and B. Giletti at Brown University for numerous fruitful discussions. This manuscript was improved by thoughtful comments from reviewers S. Hart and T. Yanosky. This work was supported by the National Institute on Environmental Health Sciences Superfund Basic Research Program Grant 5P42ES04675-06 in conjunction with the Center for Environmental Health Sciences (Massachusetts Institute of Technology).

1. Hagemeyer, J. (1993) in *Plants as Biomonitors: Indicators for Heavy Metals in the Terrestrial Environment*, ed. Markert, B. (VCH, New York), pp. 541–563.
2. Lazof, D. B., Goldsmith, J. G., Rufty, T. W., Suggs, C. & Linton, R. W. (1994) *J. Microsc. (Oxford)* **176,** 99–109.
3. Todd, P. J., McMahon, J. M. & McCandish, C. A. (1997) *Anal. Chem.* **69,** 529A–535A.
4. Tolstogouzov, A. (1995) *Microsc. Anal.* **18,** 33–34.
5. Kuhn, A. J., Schröder, W. H. & Bauch, J. (1997) *Holzforschung* **51,** 487–496.
6. Harju, L., Lill, J. O., Sarrela, K. E., Heslius, S. J., Hernberg, F. J. & Lindroos, A. (1996) *Nucl. Instrum. Methods Phys. Res. Sect. B* **109/110,** 536–541.
7. Martin, R. R., Furimsky, E., Jain, J. & Skinner, W. M. (1997) *Am. Chem. Soc. Symp. Ser.* **654,** 30–41.
8. Hoffmann, E., Lüdke, H., Scholtze, H. & Stephanowitz, H. (1994) *Fresenius' J. Anal. Chem.* **350,** 253–259.
9. Bailey, J. H. E. & Reeve, D. W. (1996) *J. Pulp Paper Sci.* **22,** J274–J278.
10. McClenahen, J. R. & Vimmerstedt, J. P. (1993) *J. Environ. Qual.* **22,** 23–32.
11. Martin, R. R., Zanin, J. P., Bensette, M. J., Lee, M. & Furimsky, E. (1997) *Can. J. For. Res.* **27,** 76–79.
12. Watmough, S. A., Hutchinson, T. C. & Evans, R. D. (1997) *Environ. Sci. Technol.* **31,** 114–118.
13. Watmough, S. A., Hutchinson, T. C. & Evans, R. D. (1998) *Environ. Sci. Technol.* **32,** 2185–2190.
14. Eklund, M. (1995) *J. Environ. Qual.* **24,** 126–131.
15. Boniette, E. A., Baes, C. F., III, & McLaughlin, S. B. (1989) *Can. J. For. Res.* **19,** 586–594.
16. Vroblesky, D. A. & Yanosky, T. M. (1990) *Groundwater* **28,** 677–684.
17. Garbe-Schönberg, C. D., Reimann, C. & Pavlov, V. A. (1997) *Environ. Geol.* **32,** 9–16.
18. Hagemeyer, J. (1995) *Trees* **9,** 200–203.
19. Trüby, P. (1995) *Angew. Bot.* **69,** 135–139.
20. Durant, J. L., Chen, J., Hemond, H. F. & Thilly, W. G. (1995) *Environ. Health Perspect.* **103,** 93–98.
21. Aurilio, A. C., Durant, J. L., Hemond, H. F. & Knox, M. L. (1995) *Water Air Soil Pollut.* **81,** 265–282.
22. Durant, J. L., Zemach, J. J. & Hemond, H. F. (1990) *Civ. Eng. Pract.* 5, 41–65.
23. Spliethoff, H. M. & Hemond, H. F. (1996) *Environ. Sci. Technol.* **30,** 121–128.
24. Gawel, J. (1996) Ph.D. Thesis (Massachusetts Inst. of Technol., Cambridge, MA).
25. Shimizu, N. & Hart, S. R. (1982) *Annu. Rev. Earth Planet. Sci.* **10,** 483–526.
26. Momoshima, N. & Bondietti, E. A. (1990) *Can. J. For. Res.* **20,** 1840–1849.
27. Crank, J. (1975) *Mathematics of Diffusion* (Oxford Univ. Press, Oxford).
28. Ellmore, G. S. & Ewers, F. W. (1986) *Am. J. Bot.* **73,** 1771–1774.